LBL-12314 c. 2
Preprint

Lawrence Berkeley Laboratory
UNIVERSITY OF CALIFORNIA

RECEIVED
LAWRENCE
BERKELEY LABORATORY
APR 6 1981
LIBRARY AND
DOCUMENTS SECTION

Materials & Molecular Research Division

Submitted to the Journal of Chemical Physics

PROTON-DEUTERIUM POLARIZATION TRANSFER IN MAGIC ANGLE SPINNING POLYCRYSTALLINE SOLIDS IN THE ROTATING FRAME

L. Müller

RECEIVED
LAWRENCE
BERKELEY LABORATORY
APR 7 1981
LIBRARY AND
DOCUMENTS SECTION

March 1981

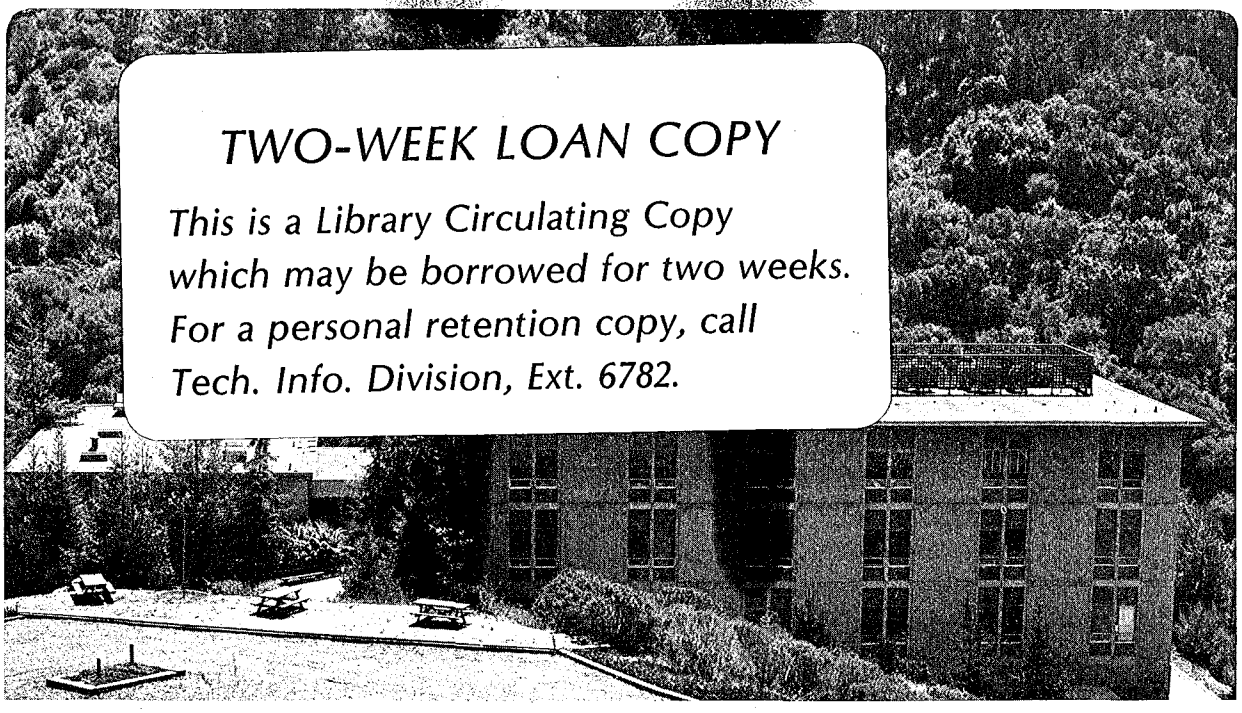

TWO-WEEK LOAN COPY

This is a Library Circulating Copy which may be borrowed for two weeks. For a personal retention copy, call Tech. Info. Division, Ext. 6782.

Prepared for the U.S. Department of Energy under Contract W-7405-ENG-48

LBL-12314 c. 2

DISCLAIMER

This document was prepared as an account of work sponsored by the United States Government. While this document is believed to contain correct information, neither the United States Government nor any agency thereof, nor the Regents of the University of California, nor any of their employees, makes any warranty, express or implied, or assumes any legal responsibility for the accuracy, completeness, or usefulness of any information, apparatus, product, or process disclosed, or represents that its use would not infringe privately owned rights. Reference herein to any specific commercial product, process, or service by its trade name, trademark, manufacturer, or otherwise, does not necessarily constitute or imply its endorsement, recommendation, or favoring by the United States Government or any agency thereof, or the Regents of the University of California. The views and opinions of authors expressed herein do not necessarily state or reflect those of the United States Government or any agency thereof or the Regents of the University of California.

PROTON-DEUTERIUM POLARIZATION TRANSFER IN MAGIC ANGLE SPINNING POLYCRYSTALLINE SOLIDS IN THE ROTATING FRAME

L. Müller
Department of Chemistry
University of California
Lawrence Berkeley Laboratory
Berkeley, California 94720

Present Address: California Institute of Technology
Department of Chemistry
Pasadena, California 91125

This work was supported by the Assistant Secretary of Fossil Energy, Office of Coal Research Liquefaction, of the Director of the U.S. Department of Energy under Contract No. W-7405-ENG-48, thru the Pittsburg Energy Center, Pittsburg, PA; and a scholarship grant from the Swiss National Science Foundation.

ABSTRACT

Proton deuterium polarization transfer in magic angle spinning polycrystalline solids in investigated, Conditions are derived under which cross polarization is possible. It is shown that standard Hartman-Hahn cross polarization works well if the quadrupolar coupling constant ω_Q^o is not too large. For large ω_Q^o a modification will be presented that makes the polarization transfer more effective. These techniques are applied to a sample of partially deuterated p-dimethoxybenzene that contains rigid aromatic and mobil aliphatic deuterium sites.

I. INTRODUCTION

Coherence transfer in the rotating frame found widespread application to enhance the sensitiviity of rare nuclei [1-3]. The relatively strong proton magnetization is spin locked in the rotating frame and brought in contact with the rare nuclei. The polarization transfer is induced by static heteronuclear dipolar interactions.

In magic angle spinning solids, however, all dipolar couplings oscillate. But Schaefer and Waugh [4,5] demonstrated that proton-carbon cross polarization is not quenched under magic angle spinning as long as the sample rotation frequency does not exceed the width of the local dipolar field. It would be attractive to use the same technique to enhance the sensitivity of deuterium in magic angle spinning solid.

Magic angle spinning high resolution deuterium NMR offers the indirect detection of proton chemical shifts without the application of multi-pulse techniques [6-9]. Deuterium has a 6.5 times lower gyromagnetic ratio than proton and substantial sensitivity gain can be expected from cross polarization in partially deuterated samples. However, for deuterium as a spin 1 nuclei with a quadrupolar interaction, rapid magic angle spinning complicates the polarization transfer. The deuterium spins under rf irradiation in the rotating frame are exposed to two orthogonal fields; the constant Zeeman field created by the rf and the electrical gradient field, which is rapidly modulated in the z-direction parallel to B_o by magic angle spinning. Thus, the effective quantization axis in the rotating frame is rapidly modulated in size and direction by the mechanical

sample rotation. In Figure 1 the deuterium transition frequencies are plotted for one rotor cycle. Strong molulation can be observed especially when the quadrupolar coupling constant ω_Q is large. It will be investigated in the following that under these conditions spin locking is possible thus if a polarization transfer takes place the generated deuterium polarization is not destroyed by sample rotation.

II. SPIN LOCKING OF DEUTERIUM POLARIZATION UNDER MAGIC ANGLE SPINNING

The effective quantization field of the deuterium spin consist of two orthogonal components, a constant rf field in the x-y plane and a rapidly oscillating quadrupole field in the z-direction of B_o. Cross polarization requires that the generated deuterium polarization can be locked in such a time dependent field. If the rotation frequency would exceed the quadrupolar coupling, the spin could not follow the quadrupolar field and just be quantized along the applied rf field. Since $\omega_Q^o = \frac{3}{4h} e^2 q Q$ can be as large as 100 kHz, this situation cannot be realized technically. What happens to the deuterium magnetization at lower spinning frequencies will be investigated in this paragraph.

The time dependence of the spin density matrix is given by: [10]

$$\dot{\rho} = -\frac{i}{h}[H,\rho] \tag{2.1}$$

where in the rotating frame

$$\frac{H}{\hbar} = \Delta I_z + \omega_1 I_x + \frac{\omega_Q(t)}{3}\,(3I_z^2 - I(I+1)) \tag{2.2}$$

and $\Delta = \omega^o - \omega$ (resonance offset)

Only for $\Delta = 0$ a simple analytical expression can be given [10]. Therefore, the following calculations are restricted to on resonance irradiation ($\Delta = 0$).

From the equation (2.1) the following set of bloch equations can be derived [10].

Definitions:

$$u_{ij} = \rho_{ij} + \rho_{ji},\ jv_{ij} = \rho_{ij} - \rho_{ji}$$

$$\omega_{ij} = \rho_{ii} - \rho_{jj} \tag{2.3}$$

$$U = (u_{12} + u_{23})2^{-3/2}$$

$$V = (v_{12} + v_{23})2^{-3/2}$$

$$W = (w_{12} + w_{23} + u_{13})/4$$

Bloch Equations:

$$\dot{U} - \omega_Q(t)V = 0 \tag{2.4}$$

$$\dot{V} + \omega_Q(t)U + 2\omega_1 W = 0$$

$$\dot{W} - 2\omega_1 V = 0$$

or in a matrix representation

$$\dot{x} = A(t)x$$

which can be transformed into [11]

$$\dot{y} = (T^{-1}AT + T^{-1}\frac{dT}{dt})y \tag{2.6}$$

where $y = T^{-1} \times T$

assuming slow time dependence, we seek the approximate solution:

$$\frac{\vec{dy}}{dt} = T^{-1}AT. \tag{2.7}$$

Eigenvalues of A are

$$E_1 = j\sqrt{\omega_Q^2 + 4\omega_1^2} \tag{2.8a}$$

$$E_2 = 0$$

$$E_3 = -j\sqrt{\omega_Q^2 + 4\omega_1^2}$$

where $j = \sqrt{-1}$

and the diagonalization matrix is:

$$T = \begin{array}{|c|c|c|} \hline \frac{\omega_Q}{\sqrt{2\gamma}} & \frac{2\omega_1}{\gamma} & \frac{\omega_Q}{\sqrt{2\gamma}} \\ \hline \frac{j}{\sqrt{2}} & 0 & \frac{-j}{\sqrt{2}} \\ \hline \frac{2\omega_1}{\sqrt{2\gamma}} & \frac{-\omega_Q}{\gamma} & \frac{2\omega_1}{\sqrt{2\gamma}} \\ \hline \end{array} \qquad (2.8b)$$

where $\gamma = (\omega_Q^2 + 4\,\omega_1^2)^{1/2}$

This yields:

$$y_1 = y_1(0)\exp\left(+j\int_o^t \gamma(t')dt'\right)$$

$$y_2 = y_2(0) \qquad (2.9)$$

$$y_3 = y_3(0)\exp\left(-j\int_o^t \gamma(t')dt'\right)$$

From Eq. (2.9) we get:

$$U(t) = \frac{2\omega_1}{\gamma^2} W_o(0)\omega_Q \left[\cos\left(\int_o^t dt'\gamma(t')\right)-1\right]$$

$$V(t) = \frac{-2\omega_1 W(0)}{\gamma} \sin\left(\int_0^t dt' \, \gamma(t')\right) \tag{2.10}$$

$$W(t) = W(0) + \frac{4\omega_1^2 \, W(0)}{\gamma^2}\left[\cos\left(\int_0^t dt' \gamma(t')\right) - 1\right]$$

For constant ω_Q Eq. (2.10) is identical with the result in [10].

The following state is constant in time.

$$Y = T^{-1}S(0) = Y_2(0) \tag{2.11}$$

We find for S(0) the following solution

$$S(0) = \begin{pmatrix} 2\omega_1 \\ 0 \\ -\omega_Q \end{pmatrix} \frac{Y_2(0)}{\gamma} \quad \text{or} \quad \frac{U(o)}{W(o)} = -\frac{2\omega_1}{\omega_Q}$$

S(0) can be considered as spin locked polarization in the effective quantization field. We define the system behaving adiabatic if S(t) = S(0) remains a constant of motion, i.e., the spin polarized can follow the time dependent external field.

Now we add the neglected term of the matrix equation [2.6] and test how much it changes the first approximated solution. The quadrupole coupling $\omega_Q(t)$ contain terms that oscillate with the one and two-fold spinner frequency ω_r [12] For simplicity and since we only want to obtain the upper limit of ω_r where the spins still can follow the change, the following simple time dependence of $\omega_Q(t)$ is defined.

$$\omega_Q(t) = \omega_Q^m \cos(\omega t) \text{ where } \omega = 2\omega_r \tag{2.12}$$

The additional term in Eq. (2,6) is;

$$T^{-1}\frac{dT}{dt} = \frac{2\omega_1\omega_Q^o\ \omega\ \sin(\omega t)}{\gamma^2(t)}\ M \tag{2.13}$$

where

$$M = \begin{array}{|c|c|c|}\hline 0 & 1 & 0 \\ \hline -1 & 0 & -1 \\ \hline 0 & 1 & 0 \\ \hline \end{array}$$

Combining this term with Eq. (2.7) yields the new differential equation

$$\frac{dy}{dt} = \begin{array}{|c|c|c|}\hline j\gamma(t) & -\nu(t) & 0 \\ \hline \nu(t) & 0 & \nu(t) \\ \hline 0 & -\nu(t) & -j\gamma(t) \\ \hline \end{array}\ y$$

where

$$\gamma(t) = (\omega_Q^2(t) + 4\omega_1^2)^{1/2}$$

$$\nu(t) = \frac{2\omega_1\omega_Q^m\ \omega\ \sin(\omega t)}{\gamma^2(t)}$$

The new eigenvalues are

$$E_1 = j(\gamma^2 + 2\nu^2)^{1/2} = j\gamma^1$$

$$E_2 = 0 \tag{2.15}$$

$$E_3 = -j(\gamma^2+2\nu^2)^{1/2} = -j\gamma^1.$$

With the new diagonalization matrix

$$R = \begin{array}{|c|c|c|} \hline \dfrac{\gamma + \gamma^1}{2\gamma^1} & \dfrac{-j\nu}{\gamma^1} & \dfrac{\gamma^1-\gamma}{2\gamma^1} \\ \hline \dfrac{-j\nu}{\gamma^1} & \dfrac{\gamma}{\gamma^1} & \dfrac{j\nu}{\gamma^1} \\ \hline \dfrac{\gamma^1 - \gamma}{2\gamma^1} & \dfrac{j\nu}{\gamma^1} & \dfrac{\gamma + \gamma^1}{2\gamma^1} \\ \hline \end{array} \qquad (2.16)$$

This transformation matrix R can be approximated by R° for $\nu \ll \gamma$.

$$R^\circ = \begin{array}{|c|c|c|} \hline 1 - \dfrac{\nu^2}{2\gamma^2} & -j\dfrac{\nu}{\gamma} & \dfrac{\nu^2}{2\gamma^2} \\ \hline -j\dfrac{\nu}{\gamma} & 1-\dfrac{\nu^2}{\gamma^2} & +j\dfrac{\nu}{\gamma} \\ \hline \dfrac{\nu^2}{2\gamma^2} & + \dfrac{i\nu}{\gamma} & 1- \dfrac{\nu^2}{2\gamma^2} \\ \hline \end{array} \qquad (2.17)$$

where $$\frac{\nu}{\gamma} = \frac{2\omega_1\, \omega_Q^m\, \omega \sin(\omega t)}{((2\omega_1)^2 + \omega_Q^{m2}\cos^2(\omega t))^{3/2}}$$

$$\left(\frac{\nu}{\gamma}\right)_{max} = \frac{\omega_Q^m \omega_r}{2\omega_1^2} \qquad (2.18)$$

Under the conditions that $2\omega_1^2 >> \omega_Q^o \omega_r$ (2.19) the correction matrix R° remains diagonal and the deuterium magnetization can follow the oscillating electric field gradient, since then $S(t) \equiv S(o)$ Eq. (2.11).

For example if $\omega_1^2 = 5\omega_Q^o \omega_r$ then constant part of the spin locked magnetization $S(o)$ is at no instant of time reduced by more than 1%. Since ω_Q^o cannot be much larger than 100 KHz and ω_r does not need to be larger than a few kiloherz to cover the spectral range of the deuterium chemical shifts, it is fortunately technically easy to generate a sufficient strong rf field to fulfill the condition (2.19).

For the off resonance irradiation modulation of the energy levels are expected to become smaller. Computer simulation of the deuterium energy levels during a rotor cycle indicate that under offresonance irradiation the modulation amplitudes are smaller than in the on resonance case (figure 1). Consequently, the condition (2.19) represents an upper level.

III. CROSS POLARIZATION DYNAMICS

a) General Consideration

In this section we shall discuss some aspects of the cross polarization spin dynamics where most spin interactions are time depended due to the mechanical sample spinning. The sample which contains N_I proton and N_S deuterium spin is placed in a large magnetic field. The high field double resonance Hamiltonian in the laboratory reference frame is then

$$H = H_I + H_S + H_{IS} + H_{rf}(t). \tag{3.1}$$

The Hamiltonian H_I is defined as

$$H_I = H_{ZI} + H_{CS}(t) + H_{II}(t) \tag{3.2}$$

where $H_{ZI} = \omega_{oI} I_Z$ represents the Zeeman Hamiltonian H_{CI} is the proton chemical shift Hamiltonian which will be neglected since it is too small, and H_{II} describes the magnetic interactions between I spins.

The deuterium spin Hamiltonian is

$$H_S = H_{ZS} + H_{CS}(t) + H_{SS}(t) + H_{SQ}(t) \tag{3.3}$$

where the first three terms have the same meaning as in Eq. (3.2). We neglect H_{SS} because the deuterium spins are diluted and their magnetic moment is smaller than that of the protons. The fourth term describes the quadrupolar interactions $H_{SQ}(t) = \frac{\omega_Q(t)}{3} (3S_Z^2 - S(S+1))$, [12]. (3.4)

If different chemical shifts in H_{CS} are present, the spins with common shifts are considered as a subsystem that is independent to others.

The Hamiltonian H_{IS} describes the interactions between I and S spin system. $H_{rf}(t)$ describes the interaction of the spins with the two applied rf fields

$$H_{rf} = 2\omega_{1I} I_X \cos(\omega_I t) + 2\omega_{IS} S_x \cos(\omega_s t) \tag{3.5}$$

where $I_x = \Sigma I_{ix}$ and $S_x = \Sigma S_{jx}$.

It is advantageous to change the reference frame into the rotating frame of the effective quantization field.

$$H^{RTU} = (RTU)^{+}H(RTU) + (RTU)^{+}\dot{(RTU)} \tag{3.6}$$

where

$$R = R_I R_S,\ R_I = e^{-i\omega_I I_z t},\ R_S = e^{-i\omega_S S_z t}$$

$$T = e^{-\frac{\pi}{2} I_y}.$$

U is real[11] and transforms deuterium spin Hamiltonian H_{SR} in its eigenbase.

$$H_S^{RT} = (\omega_S^o - \omega_S)S_z + \omega_{1S}S_x + \frac{\omega_Q(t)}{3}(3S_z^2 - S(S+1) \tag{3.7}$$

$$H_S^{RTU} = U^t H_S^{RT} U$$

In general it is impossible to give the simple expression for U. Since, however, the deuterium spin can be described as a three level system and the Hamiltonian is traceless, it can be written as

$$H_S^{RTU} = \omega_S^e S_z + \frac{\omega_Q^e}{3}(3S_z^2 - S(S+1)) \tag{3.8}$$

where ω_S^e, ω_Q^e are in general complicated expressions.

Thus Eq. (3.6) can be written as

$$H^{RTU} = \omega_{1I}I_z + \omega_S^e S_z + \frac{\omega_Q^e}{3}(3S_z^2 - S(S+1)) - 1/2\ H_{II}^o + H_{II}^{(ns)} + H_{IS}^o + H_{IS}^{(ns)}. \tag{3.9}$$

Superscript (ns) means nonsecular and ^{o} is the truncated Hamiltonian

$$H_{IT}^o = \sum_{i>j} a_{ij}(t)(\vec{I_i}\vec{I_j} - 3I_{iz}I_{jz})/2 \tag{3.10}$$

where

$$a_{ij}(t) = \gamma_I^2 \hbar r_{ij}^{-3} P_2(\cos(\theta_{ij})(t)$$

$$H_{IS} = \Sigma b_{ij} I_{ix} S_z^e \tag{3.11}$$

$$H_{IS}^o = 1/2\ b_{ij}[(I_{i_+}S_{j_-}^{1-2} + I_{i_-}S_{j_+}^{1-2})S_z^e(12) \tag{3.12a}$$

$$+(I_{i_+}S_{j_-}^{2-3} + I_{i_-}S_{j_+}^{2-3})S_z^e(23)$$

$$+(I_{i_+}S_{j_-}^{1-3} + I_{i_-}S_{j_+}^{1-3})S_z^e(13)]$$

where $S_z^e = U^+ S_z U$

where S^{i-j} are single transition operators [13,14], the diagonal parts of H_{IS}^o has been omitted since it causes only slight shifts of the energy levels, i.e., the Hartmann-Hahn condition [1].

$$b_{ij}(t) = -2\gamma_I\gamma_s hr_{ij}^{-3}P_2(\cos\theta_{ij})(t)$$

$$S_z^e(12) = (u_{12}u_{11} - u_{32}u_{31}) = S_z^e(21) \qquad (3.12b)$$

$$S_z^e(23) = (u_{13}u_{12} - u_{33}u_{32}) = S_z^e(32)$$

$$S_z^e(13) = (u_{13}u_{11} - u_{33}u_{31}) = S_z^e(31).$$

Where u_{ij} is the matrix element of U of the i^{th} row and the j^{th} column. The time evolution of the density operator can be described by equation (2.1) in the tilted rotating frame (RTU). The density operator can be expanded using projection techniques [15,16].

$$\rho_{RTU}(t) = P\,\rho_{RTU}(t) + (1-P)\,\rho_{RTU}(t) \qquad (3.13)$$

$$P = \frac{|I_z\rangle\langle I_z|}{\langle I_z,\ I_z\rangle} + \frac{|S_z\rangle\langle S_z|}{\langle S_z,\ S_z\rangle} + \frac{|S_Q\rangle\langle S_Q|}{\langle S_Q, S_Q\rangle} + \frac{|H_{II}\rangle\langle H_{II}|}{\langle H_{II},\ H_{II}\rangle}$$

based on this projection technique, Shimuzu [15] transformed the Liouville equation in the following system of linear differential equation. For the operators contained in P this equation has the form:

$$d\frac{\langle O_k(t)\rangle}{dt} = -\sum_{j=1}^{m}\int_o^t dt' tr\left[[O_k, \overset{\circ}{H}_{IS}(t)]\hat{\hat{S}}(t,t')[\overset{\circ}{H}_{IS}(t'), O_j]\right]\frac{\langle O_j(t')\rangle}{tr(O_j^+O_j)} \qquad (3.14)$$

where

$$\langle O(t)\rangle = tr\left[O^+\rho_{RTU}(t)\right] \text{ (expectation value)} \qquad (3.15)$$

and

$$S(t,t') = T\exp\left(-i\int_{t'}^{t}(1-P)\hat{H}^{RTU}(\tau)d\tau\right) \qquad (3.16)$$

in the zero'th order approximation [16] $\hat{\hat{S}}$ is replaced by:

$$\hat{\hat{S}}_o(t,t') = T\exp(-i\int_{t'}^{t} H_o^{RTU}(\tau)d\tau) \tag{3.17}$$

where H^{RTU} is the secular part of eq. (3.9) (3.18)

Even in this approximation the equations are still formidable.

Experimental results indicate that the expectation values $\langle O_j(t')\rangle$ in the integrands of eq. (3.14) change considerably slower than the inverse width of the dipolar local field or the transverse relaxation time T_c of the protons. Thus we don't make a large error in assuming the fast correlation approximation

$$\int_o^t dt' I(t,t') \langle O_j(t')\rangle = \langle O_j(t)\rangle \int_{-\infty}^{t} dt \quad I(t,t') \tag{3.19}$$

Under all these approximations we get the following equation for the variation of the deuterium Zeeman and quadrupolar polarization during the mixing process. (3.20a)

$$\begin{aligned}\frac{d\beta_{Sz}(t)}{dt} &= \frac{-1}{2}\langle\Delta\omega_{IS}^2\rangle (J_{12}(t) + J_{23}(t) + 4J_{13}(t))\beta_{Sz}(t) \\ &+ \frac{1}{2}\langle\Delta\omega_{IS}^2\rangle (J_{12}(t) + J_{23}(t) + 2J_{13}(t))\beta_{Iz}(t) \\ &- \frac{1}{2}\langle\Delta\omega_{IS}^2\rangle (J_{12}(t) - J_{23}(t))\beta_{SQ}(t) \\ &- \frac{1}{2}\langle\Delta\omega_{IS}^2\rangle (J^*_{12}(t)+J^*_{23}(t) + 2J^*_{13}(t))\ \beta_{II}(t)\end{aligned}$$

$$\frac{d\beta_{SQ}(t)}{dt} = -\frac{3}{2}\left\langle\Delta\omega_{IS}^2\right\rangle (J_{12}(t) + J_{23}(t))\beta_{SQ}(t) \qquad (3.20b)$$
$$+ \frac{1}{2}\left\langle\Delta\omega_{IS}^2\right\rangle (J_{12}(t) - J_{23}(t))\beta_{Iz}(t)$$
$$- \frac{1}{2}\left\langle\Delta\omega_{IS}^2\right\rangle (J_{12}(t) - J_{23}(t))\beta_{Sz}(t)$$
$$- \frac{1}{2}\left\langle\Delta\omega_{IS}^2\right\rangle (J_{12}^*(t) - J_{23}^*(t))\ \beta_{II}(t)$$

where

$$\left\langle\Delta\omega_{IS}^2\right\rangle = \frac{1}{4}\sum_{j=i}^{N_F} b_{ij}^2$$

$$\beta_{Sz} = \frac{\langle S_z\rangle}{tr\{S_z^2\}}\ ,\ \beta_{SQ} = \frac{\langle S_{SQ}\rangle}{tr\{S_Q^2\}}\ ,\ \beta_{II} = \frac{\langle H_{II}\rangle}{tr\{H_{II}^2\}}$$

The cross contact spectral density functions in Eq. (3.20) have the following structure:

$$J_{12}(t) = \int_{-\infty}^{t} dt' S_z^e(12)(t)\cdot S_z^e(12)(t')\cos\left(\int_{t'}^{t}(\omega_{12}(\tau) - \omega_{1I})\,d\tau\right)\cdot C(t,t')$$
$$J_{23}(t) = \int_{-\infty}^{t} dt' S_z^e(23)(t)\ S_z^e(23)(t')\cos\left(\int_{t'}^{t}(\omega_{23}(\tau) - \omega_{1I})\,d\tau\right)\cdot C(t,t') \qquad (3.21)$$
$$J_{13}(t) = \int_{-\infty}^{t} dt'\ S_z^e(13)(t)S_z^e(13)(t')\cos\left(\int_{t'}^{t}(\omega_{13}(\tau) - \omega_{1I})\ d\tau\right)\cdot C(t,t')$$

and
$$J_{ij}^*(t) = \int_{-\infty}^{t} dt' S_z^e(ij)(t)S_z^e(ij)(t')\cos\left(\int_{t'}^{t}(\omega_{ij}(t) - \omega_{1I})d\tau\right)C(t,t')(\omega_{ij}(t') - \omega_{1I})$$

For sufficiently slow rotation $J_{ij}^*(t)$ can be approximated by $J_{ij}(t)\cdot(\omega_{ij}(t) - \omega_{1I})$.

where the correlation function C(t,t') is:

$$C(t,t') = \frac{\mathrm{tr}\left(\sum b_{ij}(t) I_{i-} \hat{\hat{S}}_{oo}(t,t') \sum b_{ik}(t') I_{k+} \right)}{\mathrm{tr}\left(\sum b_{ij}^2(t) I_{i-} I_{i+} \right)} \tag{3.22}$$

where

$$\hat{\hat{S}}_{oo}(t,t') = T \exp\left(-i \int_{t'}^{t} d\tau H_{II}^{o}(\tau)\right) \tag{3.23}$$

and the oscillating deuterium transition frequencies in the frame of RTU Eq. (3.9) are:

$$\left.\begin{aligned} \omega_{12}(t) &= \omega_S^e(t) + \omega_Q^e(t) \\ \omega_{23}(t) &= \omega_S^e(t) - \omega_Q^e(t) \end{aligned}\right\} \text{ single quantum frequencies in the eigenbase of } H_S$$
$$\omega_{13}(t) = 2\omega_S^e(t) \quad \text{double quantum frequency} \tag{3.24}$$

Since the equations 3.20 are still too complicated to be analytically solved, the equation for $\frac{d\beta_I}{dt}$ and $\frac{d\beta_{II}}{dt}$ are not given. For low deuterium concentration ($N_I >> N_S$) β_{Iz} becomes constant due to the large heat capacity of the I spins. Further it can be expected that the polarization of the dipolar bath $\beta_{II}(t)$ remains small, since in rapidly spinning solids the spin lattice relaxation time of the dipolar polarization is expected to be short based on the findings of Pourquié et al., [21].

The three spectral density functions of Eq. (3.21) are caused by the three types of single transition operators in $\overset{\circ}{H}_{IS}$ in Eq. 3.12. The value of a spectral density function $J_{ij}(t)$ in Eq. (3.22) is large when the oscillation frequency $\omega_{ij} - \omega_{II} \cong 0$. particularly if the modulation amplitude of ω_{ij} is small relative to the width of $J_{ij}(t)$.

For each of the three spectral densities $J_{ij}(t)$ an optimal Hartmann-Hahn condition can be derived:

$$1. \quad \omega_{1I} = \omega_{12} \tag{3.25a}$$

$$2. \quad \omega_{1I} = \omega_{23} \tag{3.25b}$$

$$3. \quad \omega_{1I} = \omega_{13} \tag{3.25c}$$

Depending on the particular orientation of the electric field gradient acting on a Spin S, there is a sweep of the Hartmann-Hahn condition over a certain spectral range during one rotor cycle. For the setting $\omega_{1I}=\omega_{1S}$ the average of $\omega_Q(t)$ is zero thus all spins match the condition (3.25) at least once during a rotor cycle (see time evolution of ω_{12} and ω_{23} in Figure 1). For a certain offset $\omega_{1I}-\omega_{1S}$ there may be still many spins that match the conditions (3.25) at least once during a rotor cycle depending on $(\omega_Q)_{max}$ during spinning. Thus the oscillating quadrupolar coupling leads to considerable broadened Hartmann- Hahn matching curves (Figure 2).

Despite the complicatedness of the dynamic equations (3.20) it can qualitatively be concluded that in a polycrystalline sample all spins have nonzero cross relaxation rates due to the modulation of the deuterium transitions (Figure 1). Since $J_{ij}(t)$'s are always positive (eq. [3.22]), the generation of quadrupolar polarization $\beta_{SQ} S_Q$ is reduced. If in the time average $J_{12}(t) = J_{23}(t)$ then $\beta_{Sq} = 0$ and the equilibrium deuterium polarization has the form

$\rho^s_{eq} = \beta_{eq} S_z$ in the eigenbasis of the spin hamiltonian eq. (3.7) for $\omega_{1I} = \omega_{1S}$ the value of equilibrium spin temperatures β_{eq} relative to the initial amplitude of β^o_I is given by:

$$\beta_{eq} = \frac{1}{1+\varepsilon}\,\beta_I^{\circ} \qquad \varepsilon = \frac{N_S}{N_I}\,\frac{S(S+1)}{I(I+1)}\,. \tag{3.26}$$

The theoretical maximal sensitivities gain is therefore:

$$\frac{S_{cross}}{S_{90^\circ\ flip}} = \frac{\gamma_I}{\gamma_S}\,\frac{1}{1+\varepsilon} \qquad [3] \tag{3.27}$$

In the following section we shall discuss two distinct cases: on-resonance irradiation of deuterium $\omega_S^o-\omega = 0$ and magic angle off-resonance irradiation $\text{atan}\left(\frac{\omega_{1S}}{\omega_S^o-\omega_S}\right) = 54.7°$. The on-resonance irradiation approach is straightforward from the experimental point of view because the generated deuterium magnetization lays in the xy plane and yield the optimal free induction signal. Also the signal can be detected close to resonance without switching the deuterium carrier frequency, thus small instabilities of the rotor frequence has minimal impact on the resulting deuterium high resolution spectrum. The off-resonance cross polarization at $\text{atan}\,\frac{\omega_{IS}}{\omega_S^o-\omega_S} = 54.7°$ is insofar attractive that the quadrupole interaction ω_Q will be completely suppressed for $\omega_{1S} >> \omega_Q$ and the deuterium spins behave like spin I=1/2 nuclei, i.e., the cross polarization rates in Eq. (3.20) and become time independent.

III b ON-RESONANCE CROSS POLARIZATION

For $\omega_S^o - \omega = 0$ the Hamiltonian H_{RT} in Eq. (3.7) can be diagonalized analytically [13,14]. The diagonalization matrix U in Eq. 3.7 is then:

$$U = \begin{array}{|c|c|c|} \hline \frac{\cos\theta/2}{\sqrt{2}} & \frac{-1}{\sqrt{2}} & \frac{-\sin\theta/2}{\sqrt{2}} \\ \hline \sin\theta/2 & 0 & \cos\theta/2 \\ \hline \frac{\cos\theta/2}{\sqrt{2}} & \frac{1}{\sqrt{2}} & \frac{-\sin\theta/2}{\sqrt{2}} \\ \hline \end{array} \qquad 3.28$$

where

$$\sin\theta(t) = \frac{2\omega_1}{\omega_e(t)} \qquad (3.29a)$$

$$\cos\theta(t) = \frac{\omega_Q(t)}{\omega_e(t)} \qquad (3.29b)$$

$$\omega_e(t) = (\omega_Q(t) + 4\omega_{1S}^2)^{1/2}. \qquad (3.29c)$$

The eigenfrequencies ω_S^e and ω_Q^e defined in Equation 3.8 are now:

$$\omega_S^e = \frac{1}{2}\omega_e(t) \qquad (3.30)$$

$$\omega_Q^e = -\frac{1}{2}\omega_Q(t)$$

and the off-diagonal elements of S_Z in the eigenbase are: Eq. (3.12b)

$$S_Z^e(12) = -\cos\theta/2 \qquad (3.31)$$

$$S_Z^e(23) = \sin\theta/2$$

$$S_Z^e(13) = 0.$$

If the S spins are irradiated with a strong rf field ($\omega_{IS} > \omega_Q(t)_{max}$) the eigenfrequency ω_S^e approach the constant value ω_{1S} but the deuterium single quantum transition frequencies still are strongly time dependent since ω_Q

is only reduced by a factor two. As an illustration ω_{12} and ω_{23} are plotted in Figure 1c for $\omega_{1S} > \omega_Q^\circ$. However, the double quantum frequency ω_{13} becomes time independent for $\omega_{IS} >> \omega_Q$. Therefore, the double quantum matching Eq. (3.25c) can be maintained all the time for $\omega_{12} = \omega_{1S}$. Unfortunately, the prefactor $S^e_Z(13)(t)S^e(13)(t')$ in the double quantum spectral density function eq. (3.22) is exactly zero. Consequently, this process is forbidden by second order perturbation and should not give a significant contribution to the cross polarization process. For large quadrupolar coupling constants $\omega_{Qmax}(t) > \omega_L$ (local dipolar field) the spectral density function in the cross polarization Equation 3.20 are zero most of the time, and a significant slow down of the cross polarization process is expected. Practically for rigid deuterium sites where $\omega_Q^\circ \approx 130$ kHz, the upper condition holds true for most parts of a polycrystalline sample. Thus it is expected that long cross contact times are required to get the full equilibrium polarization eq. (3.26-27) for rigid deuterium spins.

Even with the knowledge of the prefactors (eq. 3.31) in the spectral density functions in eq. 3.22 it is very difficult to derive the exact time evolution of the deuterium polarization (β_{Sz} and β_{SQ}). Furthermore, in a polycrystalline sample each crystal orientation has its own cross polarization rate. In the following we restrict ourself to investigating what the deuterium polarization is when the system reaches the thermodynamic equilibrium.

Equation 3.20 shows that the cross polarization rate for β_{SQ} is $J_{12}(t)-J_{23}(t)$. Therefore if in the time average $J_{12}(t) = J_{23}(t)$ the equilibrium value of $\beta_{SQ} = 0$. In Figure 3a and c the prefactors of the spectral density function in eq. (3.22) are approximated by $(S^e_z(ij)(t)S^e_z(ij)(t') \rightarrow S^2_z(ij)(t))$ and plotted (3.33) for tow different quadrupolar coupling constants. In the region of the crossing points $\omega_Q(t)$ is small and changes sign thus $S^e_z(12)$ and $S^e_z(23)$ are symmetric

and have the same average value. Thus for $\omega_{II} = \omega_{IS}$ the time average of $J_{12}(t)$ and $J_{13}(t)$ is equal in the region where $\omega_Q(t)$ is small. This is also the region when most of the cross polarization takes place. It can therefore be expected that β_{SQ} remains small under the condition $\omega_{1I} = \omega_{1S}$. Then the equilibrium density operator has the form

$$\rho_{eq} = \beta_{eq}(I_z+S_z) \tag{3.32}$$

β_{eq} is given in eq. (3.28a). Thus the proton deuterium cross contact leads to a pure Zeeman polarization on the deuterium side; however, this happens in the eigenbase of the spin hamiltonian eq. (3.7). But observed is the polarization in the rotating frame of the detector frequency ω_S. The Zeeman polarization has to be transformed into this frame.

$$S_{S_z} = \beta_{S_z} U S_z U^T = \tag{3.33a}$$

$$= \beta_{S_z} (\sin\theta S_x + \tfrac{1}{4}\cos\theta(S_+^2 + S_-^2) + \tfrac{1}{2}\cos\theta (3S_z^2 - S(S+1))$$

$$S_{S_Q} = \beta_{S_Q} U S_Q U^T = -\tfrac{1}{2}(3S_z^2 - S(S+1)) + \tfrac{3}{4}(S_+^2 + S_-^2). \tag{3.33b}$$

This equation shows that the population differences in the eigenbase of the Hamiltonian are a composition of single quantum (S_x), double quantum ($S_+^2 + S_-^2$) and quadrupolar polarization $(3S_z^2-S)S+1))$ [17] depending on the ration ω_{1S}/ω_Q.

Under the assumption that the equilibrium polarization is described by eq. (3.32) we calculated the observed single quantum polarization $S_{SQ} = \langle S_x \rangle$ relative to the total deuterium polarization of eq. (32) as a function of the deuterium rf field strength ω_{1S} for a given ω_Q^o in a perfect powder (Figure 4). The result is surprising; the

the portion of single quantum polarization grows very quickly, for $\omega_{1S} = 0.25\ \omega_Q^\circ$ it reaches already three quarters of the total polarization.

In a nonspinning solid the situation is different, ω_Q is constant and only one Harmann-Hahn condition in eq. (3.25) can be matched. (3.36a)

For $\omega_{1S} > \omega_Q$ under both matching conditions (eq. 3.35) the polarization transfer rates are equal because $S_z^{e2}(12) = S_z^{e2}(23) = \cos^2 45$ (see eq. 3.32 and 3.27). In this case only single quantum polarization is generated. However, for $\omega_{1S} < \omega_Q$ the cross polarization rate eq. (3.27) becomes very small under one condition in 3.26. But under the other condition in 3.25 the cross polarization rate becomes twice as large as for single quantum polarization since here $S_z^{e2}(12) = \cos\theta^2 = 1$ and only double quantum polariztion is generated as outlined below [19]. In a nonspinning solid where $\omega_{1S} < \omega_Q$ and $\omega_Q > o$

$$S_{eq} = \beta_z\ S^{1-2} \text{ in the eigenbase of } H_S \text{ (eq. 3.7) where}$$

$$S_z^{1-2} = \frac{1}{4}\ (S_z + S_Q) \tag{3.34}$$

backtransformed into the rotating reference frame

$$S_{eq} = U\beta S_z^{1-2}\ U^t = \frac{\beta}{4}\ (\sin\theta S_x + \frac{1}{4}(3+\cos\theta)(S_x^2 + S_-^2) + \frac{1}{2}(\cos\theta - 1)(3S_z^2 - S(S+1)) \tag{3.35}$$

and for $\omega_Q >> \omega_{1S}$ $\cos\theta \to 1$ and only double quantum polarization is generated

$$S_{eq}(\omega_Q >> \omega_{1S}) = \frac{\beta}{4}\ (S_+^2 + S_-^2) \tag{3.36}$$

IIIc MAGIC ANGLE OFF-RESONANCE CROSS POLARIZATION

It is well known that quantization of spins at a tilted axix (20), which is inclined by the magic angle θ_m=atan$\sqrt{2}$ permit the suppression of certain spin-spin interactions like homonuclear dipolar coupling. This can be achieved by off resonance irradiation maintaining the following relation between rf field amplitude and resonance offset $\tan\theta_m = \frac{\omega_1}{\omega_o-\omega} = \sqrt{2}$. Transformation of the deuterium Hamiltonian in eq. 3.7 into the frame of this effective Zeeman field we get:

$$H_S^{RT} = T^t H_{SR} T = \omega_{eff} S_z + \frac{\omega_Q}{3} \frac{1}{2}(3\cos^2\theta-1)(3S_z^2-S(S+1)) + \omega_Q\left(-\frac{1}{2}\sin 2\theta(S_z S_x + S_x S_z) + \frac{1}{4}\sin^2\theta(S_+^2 + S_-^2)\right) \qquad (3.37)$$

where $T = e^{-i\theta S_y}$

$$\omega_{eff} = ((\omega_S^\circ-\omega_S)^2 + \omega_{1S}^2)^{1/2}.$$

For $\omega_{eff} >> \omega_Q$ the last two terms in eq. (3.27) become nonsecular and have diminishing influence on the time evolution. Thus for $\omega_{eff} >> \omega_Q$ and $\theta=\theta_m$ the effective deuterium spin Hamiltonian is reduced to

$$H_S^{RT^\circ} = \omega_{eff} S_z \qquad (3.38)$$

Under this condition the cross relaxation rates in eq.(3.20) become time independent and $J_{12} = J_{23}$ and $J_{13} = 0$. Thus the deuterium spin behaves like spin 1/2 nuclei, where it has been shown that cross polarization works well under rapid magic angle spinning [4,5].

However, for rigid, immobile deuterium sites where $\omega_Q^o \simeq 130$kHz it is practically impossible to fulfill the condition $\omega_{1S} >> \omega_Q$ for all orientations in a powder, rf field strengths of several hundred kHz would be required. In realistic cases $\omega_{1s} \simeq \omega_Q$ for a substantial part of the rotating powder. Unfortunately, in this case it is very difficult to diagonalized the deuterium spin Hamiltonian and no simple expression for the diagonalization matrix U in eq. (3.7) can be given. We restrict ourself to present numerical calculations for selected arbitrary deuterium orientations (angle between the principal axis of the quadrupole tensor and the rotor axis $\beta = 70°$). In Figure 1b the two deuterium frequency $\omega_{12}(t)$ and $\omega_{23}(t)$ are calculated for one rotor cycle for $\omega_Q^o = 130$ kHz, $\omega_{1S} = 34$ kHz, $\beta = 70$ i.e., ($\omega_{Q\ max} >> \omega_{1S}$ and compared to the on resonance case, it is seen that the modulation amplitude is already distinctly reduced for the setting $\omega_{1I} = \omega_{1S} = 34$ kHz and practically always one H.H. condition eq. (3.25) is fulfilled.

In Figure 1d the deuterium frequencies are calculated for $\omega_Q = 33.1$ and $\omega_{1S} = 34$ kHz ($\omega_Q \simeq \omega_{1S}$) for the same orientation β and compared to the on resonance case. We see that for the on resonance irradiation the deuterium frequencies ω_{12} and ω_{23} still strongly oscillate whilst under magic angle irradiation they become almost time independent. Also of importance are the prefactors $\left(S_z^e(ij)^2\right)$ of the cross polarization spectral density functions in eq. (3.22). In Figure $\left(S_z^e(ij)^2\right)$ are plotted for the time of one rotor cycle. The same parameters are used as for the Figure 1 calculations. Figure 3b and 3a represent the off resonance and on resonance case respectively for $\omega_Q^o = 130$, $\omega_{1S} = 34$, $\beta = 70°$. We see in 3b that the coefficients for the single quantum spectral density functions $J_{12}(t)$, $J_{23}(t)$ are large in the

region where $\omega_Q \tilde{=} 0$ (compare with Figure 1). Also remarkable is that the forbidden double quantum process induced by $J_{13}(t)$ with the prefactor $\left(S_z^e(13)^2\right)$ becomes detectably large. Thus the double quantum matching (Fig. 3.25c) $\omega_{1I}=2\omega_S^e$ leads to a cross polarization.

Increasing of the ratio $\omega_{IS}/\omega_Q^\circ$ has the following effect as illustrated in Figure 3c and 3d. The oscillation amplitudes of the prefactors become smaller for both cases (on-and off-resonance irradiation). The prefactor $\left(S_z^e(13)^2\right)$ for the double quamtum process is reduced but still detectable at $\omega_{1S} \tilde{=} \omega_Q$. From the reduction of the modulation in Figure 1b, 1d it can be expected that cross polarization in the off-resonance case is faster than under on-resonance irradiation. Numerical calculation at particular points show that the the single quantum coherence grows in the same way as shown in Figure 4 for the on-resonance case. However, the equilibrium value is reduced by the factor $\sin(\theta_m)$ since the polarization is tilted out of the xy plane. It can generally be concluded that under magic angle off-resonance irradiation of the deuterium spins the cross polarization process is expected to become faster, but the equilibrium transverse deuterium magnetization is reduced relative to the value obtained by on-resonance cross polarization.

IV EXPERIMENTAL

All cross polarization experiments have been performed on a home built spectrometer at $\frac{\omega^\circ}{2\pi}$(proton)= 182 MHz. The NMR probe was equipped with a Alla type sample spinner [22] with a double tuned single coil circuit [23].

The sample rotation was monitored optically. Further the home made pulse programmer was synchronized to the sample rotation in order to perform cross polarization and detection of the cross polarized deuterium signal synchronously to the sample rotation.

Cross polarization experiments were performed in a standard way [1-3] by spin locking of proton magnetization under simultaneous irradiation of the deuterium. The cross contact time was always incremented in steps of full spinner rotor cycles. In the on-resonance experiments, both deuterium and protons were irradiated near resonance, while in the off-resonance experiments deuterium was irradiated off-resonance such that $\text{atan} \frac{\omega_{1S}}{\omega_S^o - \omega_S} = 54.7$.

Detected were the peaks of the rotational echoes after the cross contact. The detection of these echoes with the reference frequency far off-resonance would magnify the effects of small spinning instabilities. Thus in the off-resonance experiments the deuterium frequency had to be switched coherently to on-resonance after the cross contact for detection.

V. EXPERIMENTAL RESULTS

On resonance and magic angle off-resonance proton-deuterium cross polarization experiments were performed on a sample of partially deuterated p-dimethoxybenzene. Other samples also have been used [9] but dimethyloxybenzene turned out to be most illustrative since it contains rigid deuterium sites with large quadrupolar couplings ω_Q^o=130kHz on the benzene ring and a mobile site on the methyl group with the partially averaged ω_Q^o=33.1 kHz. In Figure 5 the signal gain due to the different types of cross polarization is demonstrated. In 5a the spectrum obtained by a regular deuterium 90° pulse experiment is shown. In 6b on resonance cross polarization was applied with $\omega_{1I}=\omega_{Seff}$=34kHz.

Remarkable is that the measured signal enhancement relative to a regular deuterium 90° flip experiment is larger than the theoretical value (Table 1). This is due to the fact that during the application of a 90 pulse the deuterium quadrupole coupling causes a decay of the deuterium transverse magnetization. In a cross polarization experiment on the other hand all generated transverse magnetization is in phase over the entire polycrystalline sample. In the off-resonance cross polarization the deuterium magnetization is tilted out of the xy-plane causing a reduced observed signal of 81.7%. According to Figure 6 and Table 1 the methyl peak intensity indeed decreases by moving from on-resonance to off-resonance cross polarization.

The aromatic peaks however become more intense in the off-resonance cross polarization experiments (Fig.6). This indicates that the methyl deuterium whose

quadrupole coupling constant ω_Q^o is smaller than ω_{Seff} have reached the equilibrium polarization during the cross contact of about 16 msec in all experiments (Figure 5), but the aromatic deuterium whose ω_Q^o is considerably larger than ω_{Seff} do not reach the equilibrium polarization in the on-resonance experiment.

In Figure 6 the proton enhanced deuterium signal is measured as a function of the cross contact time which was increased in steps of full rotor cycles. The magnetization $M_j(t)$ in Figure (6) refers to the peak (j) in Figure (5). Figure 6a, 6b show qualitatively what we expect from the theoretical model outlined in the previous chapter. Off-resonance irradiation of the deuterium increases the cross polarization rate and increase of the rf field strength maintaining magic angle off-resonance irradiation further increases the transfer rate due to the quenching of the modulation amplitude of the deuterium frequencies in the rotating frame (see Figure 1). Since however $\omega_Q^o >> \omega_{Seff}$ for the aromatic sites the polarization of those is considerable slower than for the methyl group. Figure 6c also shows that on-resonance polarization is slower for the methyl deuterium but yield a high equilibrium value than magic angle off-resonance polarization. It also demonstrates that the equilibrium magnetization does not change by an increase of the effective Zeeman field strength ω_{Seff} if it is already larger than ω_Q^o. Figure 6a, 6b shows that the increase of ω_{Seff} from 36kHz to 49 kHz cause only a small increase of the equilibrium polarization of the aromatic sites in agreement with the curve in Figure 4.

The matching curves shown in Figure 2 indicate that the rigid deuterium sites with large ω_Q^o should have a considerable larger Hartmann-Hahn matching

range i.e., the proton enhanced signal should be insensitive for large mismatches, $\omega_{1H}-\omega_{Seff}$. The experimental results in Figure 7 confirm these expectations. For on-resonance cross polarization the aromatic deuterium (Δ) have a considerable broader matching range than the methyl deuterium. Off-resonance irradiation asymmetrically narrows the matching curves on the lower frequency side (ie., strong signal decrease for $\omega_{Seff}>\omega_{1H}$). This agrees with the results on Figure 1, which shows that off-resonance irradiation reduces the modulation amplitude asymmetrically.

CONCLUSION

Proton-deuterium polarization transfer in the rotating frame works well in a magic angle spinning polycrystalline solid. It probably works much better than in a nonspinning solid [18,19] since there is a wide spread of matching conditions due to the large ω_Q^o. Spinning modulates the deuterium frequencies in such a way that all nuclei match the HH condition eq. (3.25) at least once per sample rotation for $\omega_{1H}=\omega_{Seff}$. The experimental results indicate that cross polarization under on resonance irradiation of the deuterium transitions works well if the quadrupolar coupling constant is small enough (Figure 5b). For large ω_Q^o an excessive long contact time is required during which the rf circuitry may overheat. Thus magic angle off-resonance cross polarization offers an elegant alternative for spins with a large quadrupole coupling constants even if the achievable rf field strength ω_{1S} is considerably smaller than ω_Q^o. It has also been demonstrated that already at moderate level of ω_{1S} most of the proton enhanced signal goes into deuterium single quantum coherence (transverse magnetization). Thus an increase of ω_{1S} does only increase the transfer

rate especially in the off-resonance case but does not increase much the equilibrium yield of transferred polarization. The spectra of the partially deuterated p- dimethoxybenzene show considerably narrower lines than spectra of perdeuterated samples (Figure 8). This phenomenon was also encountered with other partially deuterated compounds. This is due to a reduction of the homonuclear dipolar deuterium interaction by dilution. Consequently, cross polarization may be used as a tool to increase resolution in deuterium high resolution spectra. Instead of perdeuterated compounds partially deuterated compounds can be used applying cross polarization techniques. In this way the same sensitivity is obtained as in perdeuterated samples but with increased resolution.

It can be concluded that proton deuterium cross polarization in the rotating frame works well if the derived adiatatic condition eq. (2.19) is not violated. This condition is easy to fulfill since the deuterium quadrupole coupling constant is limited to about 100 kHz and the spinning frequency is not required to exceed few kilohertz if rotation synchroneous sampling is applied, since the deuterium chemical shift spread is small even at very high magnetic fields. We have shown that on resonance cross polarization is most suitable for small quadrupolar coupling constants (motional averaged) whilst the magic-angle off-resonance cross polarization is to be preferred when ω_Q^o is very large (rigid deuterium positions, $\omega_Q^o \simeq 130$ kHz).

Figure 1 The two deuterium transition frequencies ω_{12} and ω_{23} are calculated for the time of one rotor cycle in a magic angle spinning solid under on and off resonance rf irradiation and different quadrupole coupling constants.

a) ω_Q^o = 130 kHz, ω_{Seff} = 34 kHz, on resonance

b) ω_Q^o = 130 kHz, ω_{Seff} = 34 kHz, magic angle off resonance irradiation.

c) ω_Q^o = 33.1 kHz, ω_{Seff} = 34 kHz, on resonance

d) ω_Q^o = 33.1 kHz, ω_{Seff} = 34 kHz magic angle off resonance

Figure 2 Plotted are the number of spins that matche the Hartmann-Hahn conditions (eq. 3.25 a,b) at least once during one spinner rotor cycle, under on resonance irradiation.

a) $\omega_Q^o/2\pi$ = 130 kHz, ω_{1S} = 34 kHz.

b) $\omega_Q^o/2\pi$ = 33.1 kHz, ω_{1S} = 34 kHz.

The distinct tails of the curve lay in the region where only one of the conditions 3.26 can be matched. The deuterium rf field strength is constant and the proton rf field amplitude varies.

Figure 3 The square of the coefficients in eq. 3.12b, which are identical with the prefactors $S_z^e(ij)(t)$ in the spectral density functions eq. 3.21 for slow rotation, are numerically calculated for one rotor cycle.

a) On resonance irradiation, ω_Q^o = 130 kHz,

ω_{1s} = 34 kHz, β = 70.

b) Magic angle off resonance irradiation

same parameters as in 3a.

c) On resonance irradition

ω_Q^o = 33.1 kHz, ω_{Seff} = 34 kHz, β = 70.

d) Off resonance irradiation, same

parameters as in 3c.

Figure 4 The relative amount of single quantum coherence of the total cross polarization deuterium signal is plotted as a function of the deuterium rf field strength assuming an isotropically distributed powder. For $\omega_{1S} = 0.75\ \omega_Q^o$ already 93% of the proton enhanced deuterium signal is single quantum coherence (transverse magnetization).

Figure 5 The signal gain due to proton deuterium cross polarization is shown with a sample of part deuterated dimethoxybenzene. In all four experiments the rotation frequency ν_r = 1070 Hz. Sample weight: 200 mgr, cross contact time 16 τ_r. number of scans per experiment: 10.

a) This spectrum is obtained by detecting the deuterium FID generated by a 90° rf pulse.

b) On resonance cross polarization $\omega_{1S} = 34$ kHz $= \omega_{1I}$,

c) Off-resonance cross polarization $\omega_{Seff} = 34$ kHz $= \omega_{1I}$

$\tau_{cr} = 16\tau_r$.

d) Off resonance corss polarization $\omega_{Seff} = 49$ kHz $= \omega_{1I}$

$\tau_{cr} = 16\tau_r$.

Figure 6 The deuterium signal gain is recorded as a function of the cross contact time $t = n\,\tau_r$.

△: magic angle off-resonance cross polarization, $\omega_{Seff} = 49$ kHz $= \omega_{1I}$.

□: magic angle off-resonance cross polarization, $\omega_{Seff} = 34$ kHz $= \omega_{1I}$.

○: on resonance cross polarization, $\omega_{Seff} = \omega_{1S} = \omega_{1I} = 34$ kHz.

6a) for the aromatic peak one (see Figure 52).

6b) for the aromatic peak two.

6c) for the methyl-peak three.

Number of accumulations per point: 10

Relaxation delay between to experiments: 50 sec., spinning frequency = 1070 Hz.

Figure 7 The proton-deuterium cross polarized signal has been measured for a series of different proton rf field strengths keeping constant the deuterium effective Zeeman field strength ω_{Seff}.

O: magic angle off-resonance polarization $\omega_{Seff} = ((\omega_S^o-\omega_S)^2 + \omega_{1s}2)^{1/2} = 34$ kHz, atan $\frac{\omega_{1S}}{\omega_{S-}^o\omega} = \sqrt{2}$.

Δ: on resonance cross polarization $\omega_{Seff} = \omega_{1S} = 34$ kHz.

7a The average of the two aromatic peaks (Figure 5a, peak 1 and 2).

7b Methyl peak (Figure 5a, peak 3) cross contact time $\tau_{cr} = 16\ \tau_r$.

Figure 8 The resolution enhancement by cross polarization is demonstrated.

8a Magic angle spinning high resolution deuterium spectrum of part. deuterated p-dimethoxybenzene; signal obtained by proton deuterium cross polarization.

8b High resolution spectrum of perdeuterated p-dimethoxybenzene.

REFERENCES

1) S.R. Hartmann and E.L. Hahn, Phys. Rev. 128, 2042 (1962).

2) A.Pines, M.G. Gibby and J.S. Waugh, J. Chem. Phys. 59, 569 (1973).

3) M. Mehring, High Resolution NMR Spectroscopy in Solids, Springer Verlag, Berlin, 1976.

4) J. Schaefer, E.O. Stejskal, J. Amer. Chem. Soc. 98, 1931 (1976).

5) E.O. Stejskal, J. Schafer and J.S. Waugh, J. Magn. Reson. 28, 105, (1977).

6. J.L. Ackerman, R. Eckman and A. Pines, Chem. Phys. 42, 423 (1979).

7) M. Alla, R. Eckman and A. Pines, Chem. Phys. Lett., 71, 148 (1980).

8) R. Eckman, L. Müller and A. Pines, Chem. Phys. Lett. 74, 376 (1980).

9) L. Müller, R.Eckman and A. Pines, Chem. Phys. Lett. 76, 149 (1980).

10a) D.G. Gold and E.L. Hahn, Lecture Notes, Ampere Summer School IV, Pula, Yugoslavia (1976).

10b) R.G. Brewer and E.L. Hahn, Phys. Rev. A11, 1641 (1975).

11) F.R. Gantmacher, Matrix Theory, II p.113, Chelsea Publishing Company (1974).

12) M. Matti Maricq and J.S. Waugh, J. Chem. Phys. 70, 3300 (1979).

13a) S. Vega and A. Pines, J. Chem. Phys. 66, 5624 (1977).

13b) S. Vega, J. Chem. Phys. 68, 5518 (1978).

14) A. Wokaun and R.R. Ernst, J. Chem. Phys. 67, 1752 (1977).

15) T. Shimizu, J. Phys. Soc., Japan 28, 811 (1970).

16) D.E. Demco, J. Tegenfeldt and J.S. Waugh, Phys. Rev. B11, 4133 (1975).

17) W. de Boer, M. Borghini, K. Morimoto, T.O. Niinikosko and F. Udo, Phys. Lett. 46A, 143 (1973).

17b) W. de Boer, Phys. Rev. B12, 828 (1975).

18) S. Vega, T.W. Shattuck and A. Pines, Phys. Rev., in press.

19) P. Brunner, M. Reinhold and R.R. Ernst, J. Chem. Phys. 73, 1986 (1980).

20) M. Lee and W.I. Goldburg, Phys, Rev. 140, A1261 (1965).

21) J.F.J.M. Pourquié and R.A. Wind, Phys. Lett. 55A, 347 (1976).

22) R. Eckman, M. Alla and A. Pines, J. Magn. Reson, in press.

23) V.R. Cross, R.K. Hester and J.S. Waugh, Rev. Sci. Instrum. 47, 1486 (1976).

ACKNOWLEDGEMENT

The author acknowledges the scholarship granted by the Swiss National Science Foundation. He also strongly appreciates the support from Professor A. Pines. Many thanks go to S. Wolfe for the preparation of the samples and to J. Murdoch for his permission to use portions of his software. The author would also like to thank R. Eckman for his instruction in the art of accurate spinning.

This work was supported by the Assistant Secretary of Fossil Energy, Office of Coal Research Liquefaction, of the Director of the U.S. Department of Energy under Contract No. W-7405-ENG-48 thru the Pittsburg Energy Center, Pittsburg, PA; and a scholarship grant from the Swiss National Science Foundation.

TABLE 1

Experimental:

$\omega_{Seff}/2\pi$ [kHz]	Resonance Offset [kHz]	Peak 1 $S^{CP}/S°$	Peak 2 $S^{CP}/S°$	Peak 3 $S^{CP}/S°$
34	0	1.82	1.76	3.03
34	19.63	2	2.29	2.72
49	28.9	2.52	2.57	2.75

Theoretical: (eq.(3.27))

$S^{CP}/S°$ (on resonance) = 2.34

$S^{CP}/S°$ (off-resonance) = 1.91

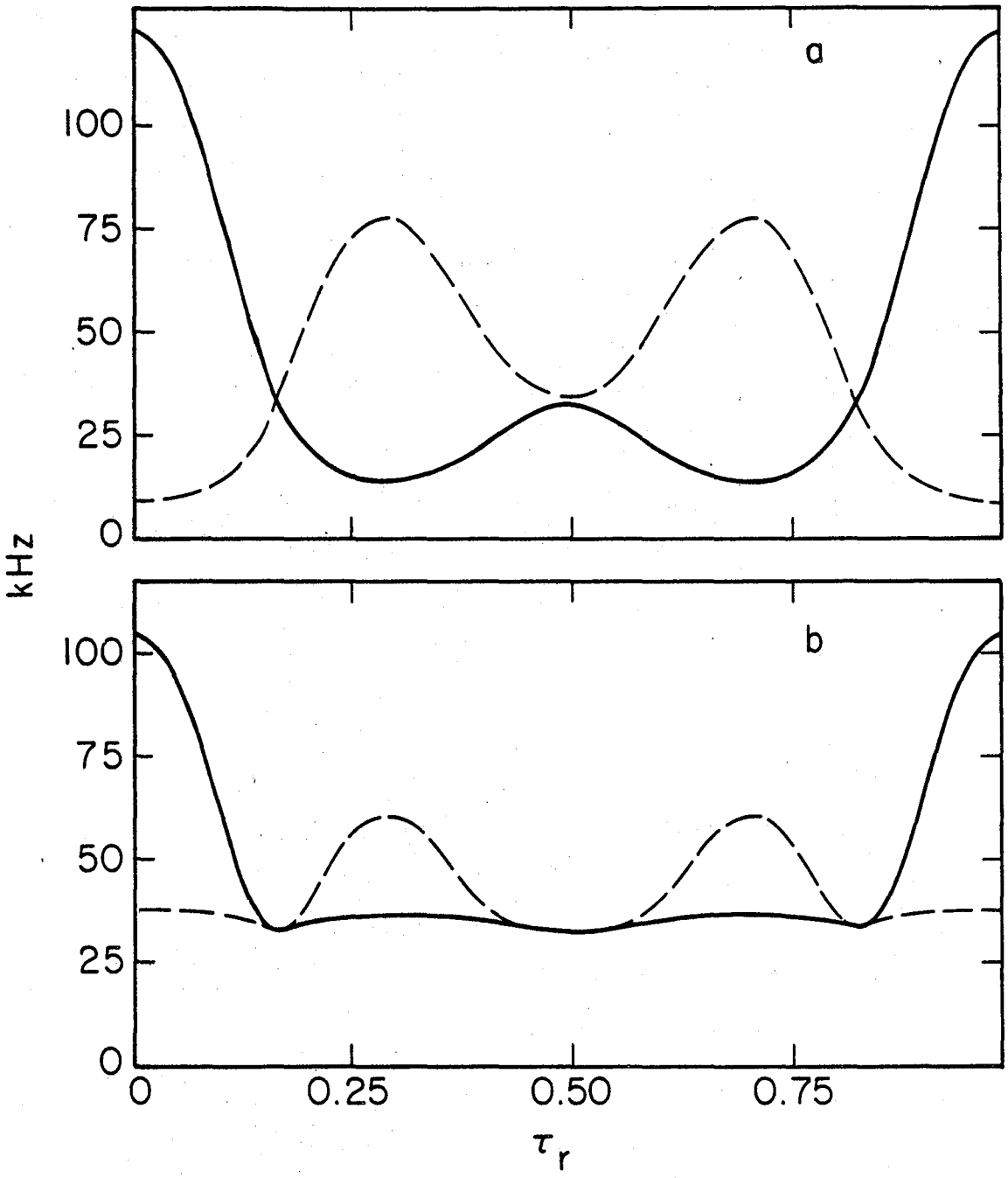

Fig. 1a,b

XBL 805-9687

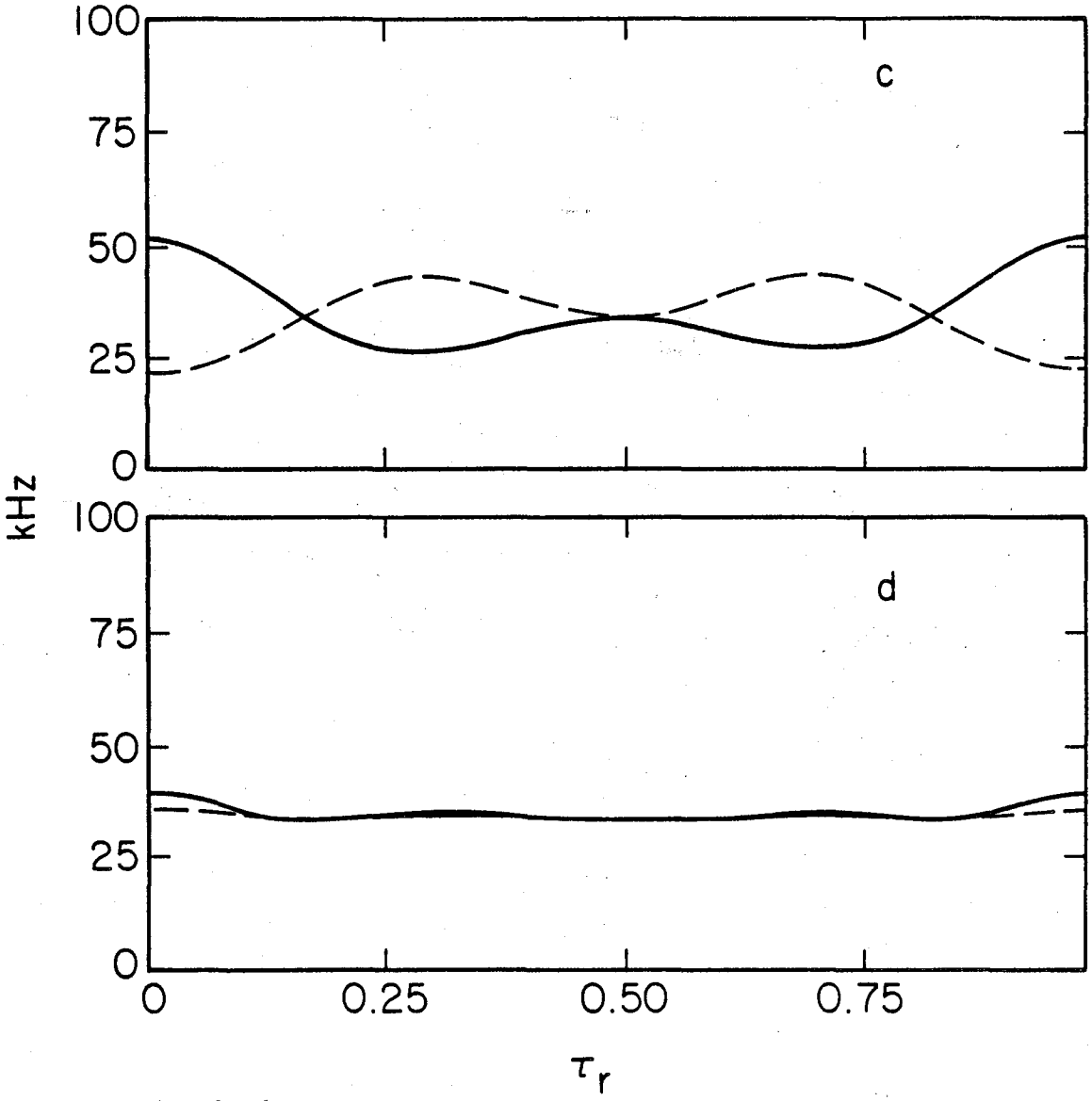

Fig. 1c,d

XBL 805-9686

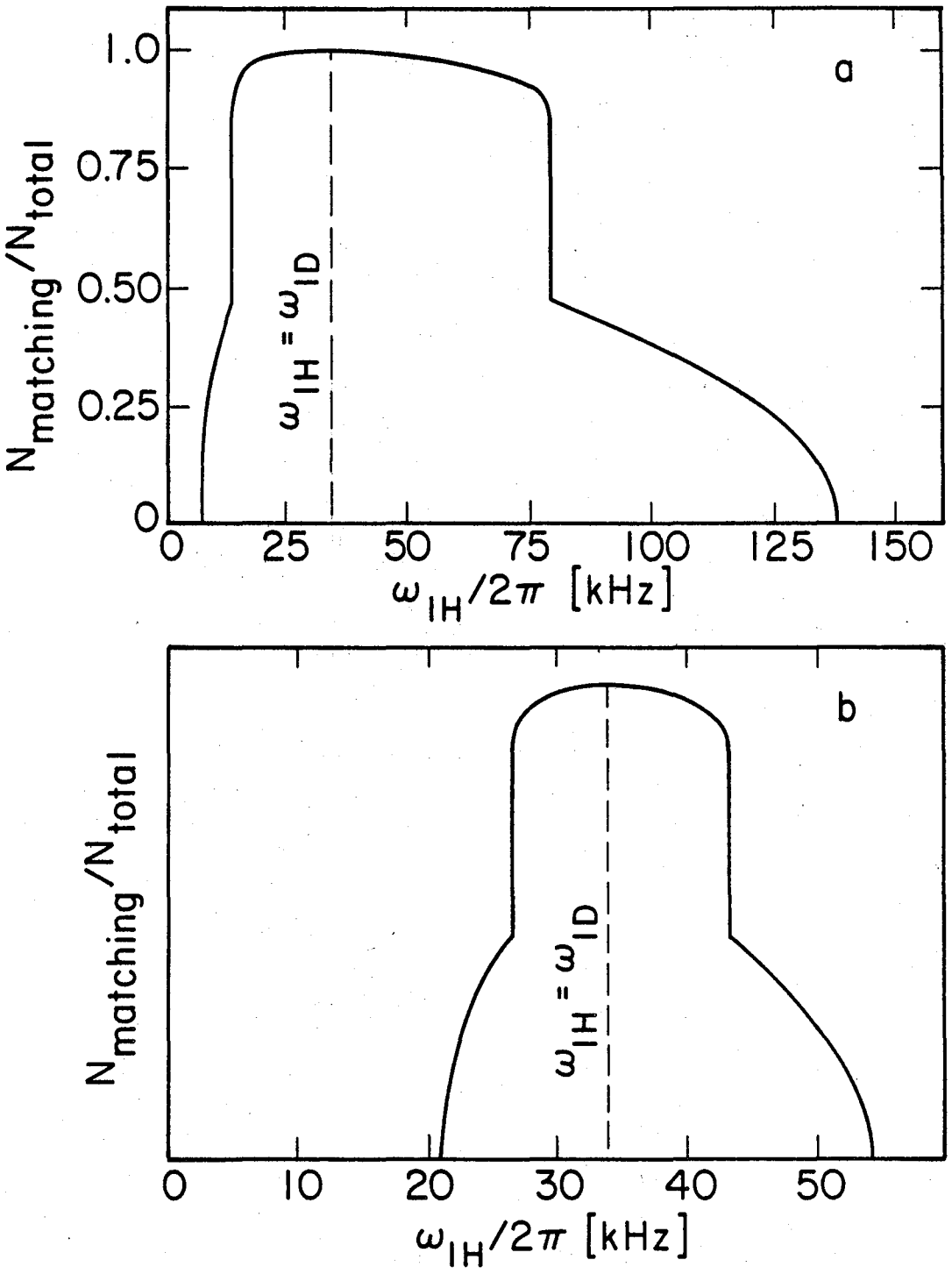

Fig. 2

XBL 805-9691

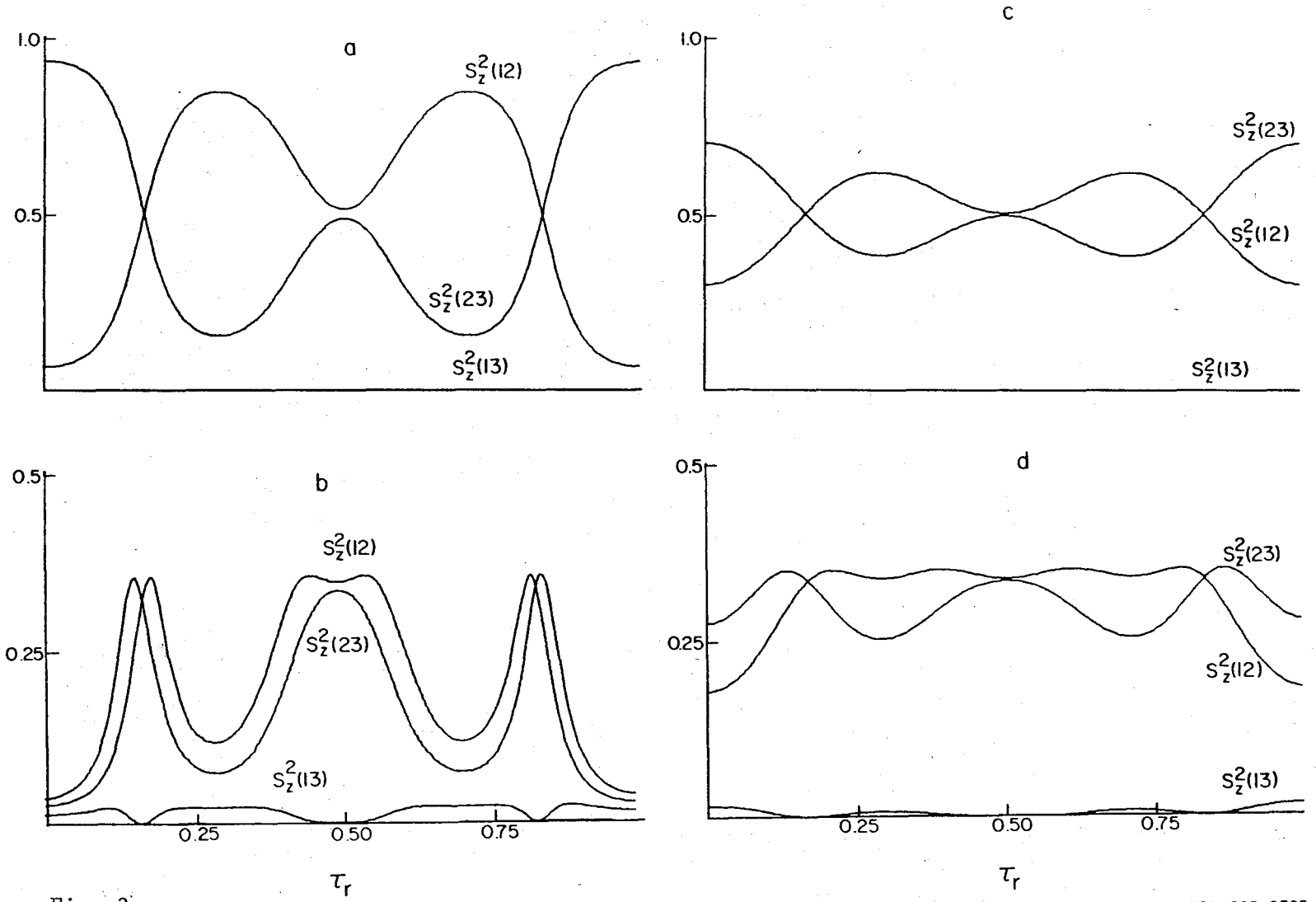

Fig. 3

XBL 805-9785

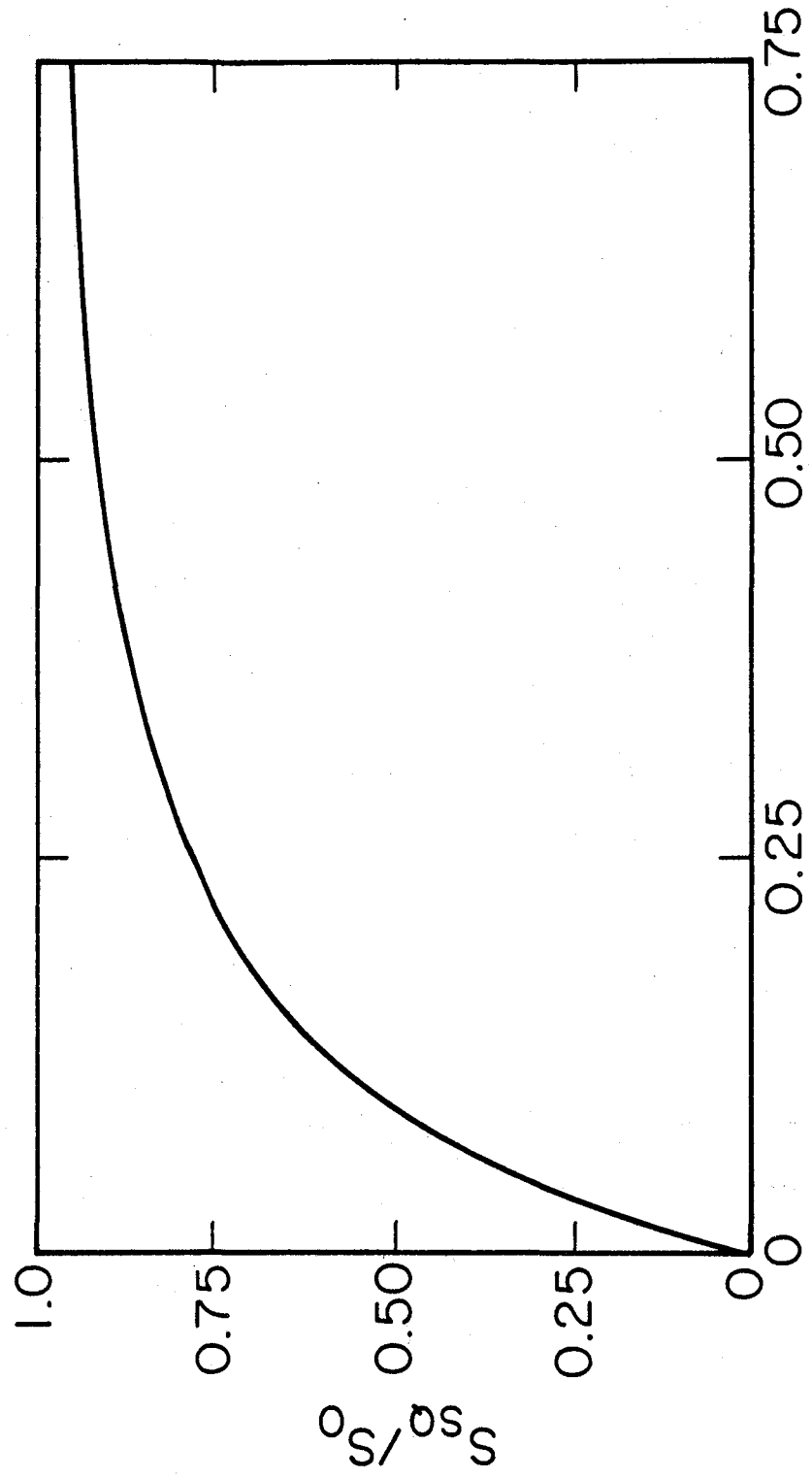

XBL 805-9688

Fig. 4

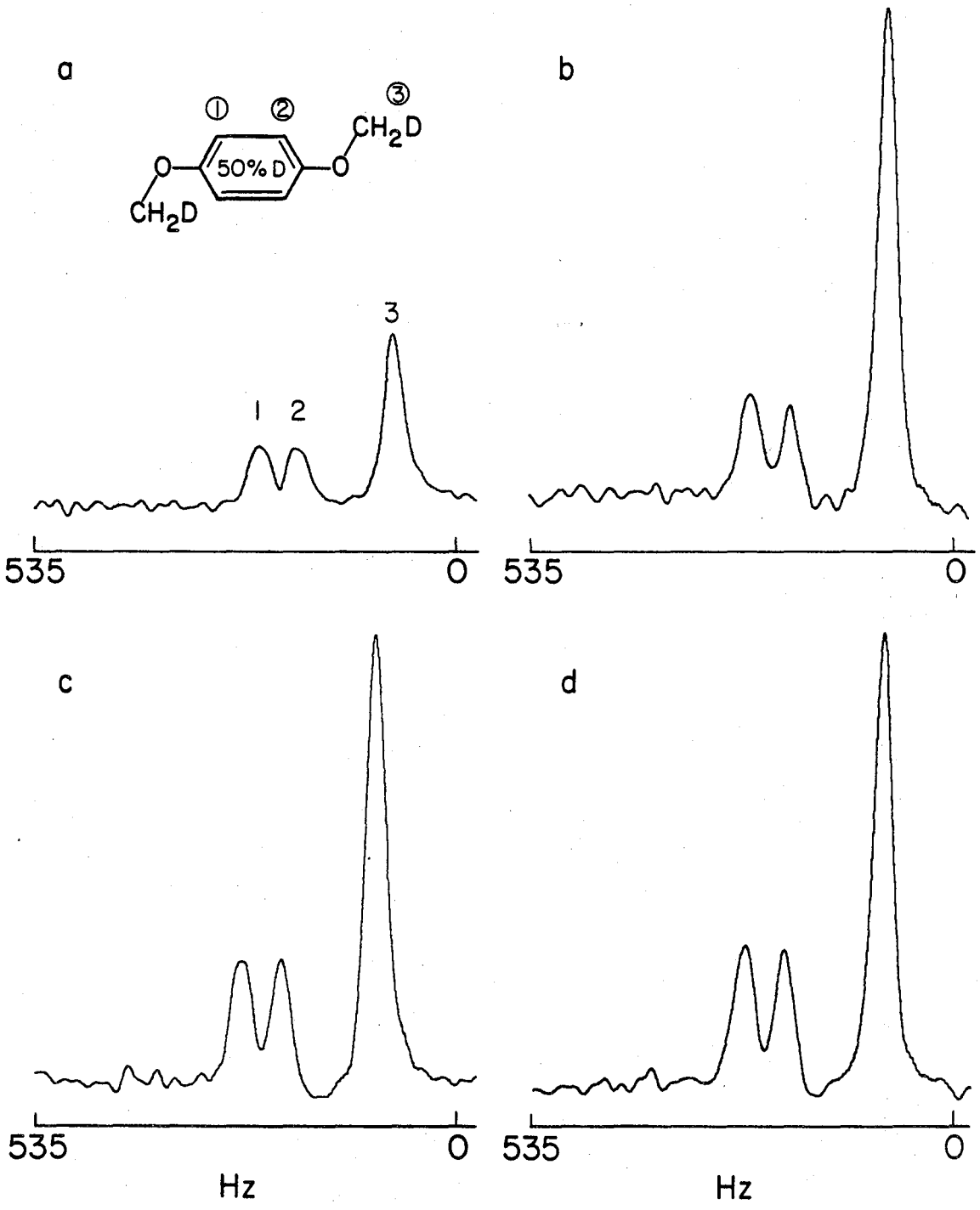

Fig. 5

XBL 805-9689

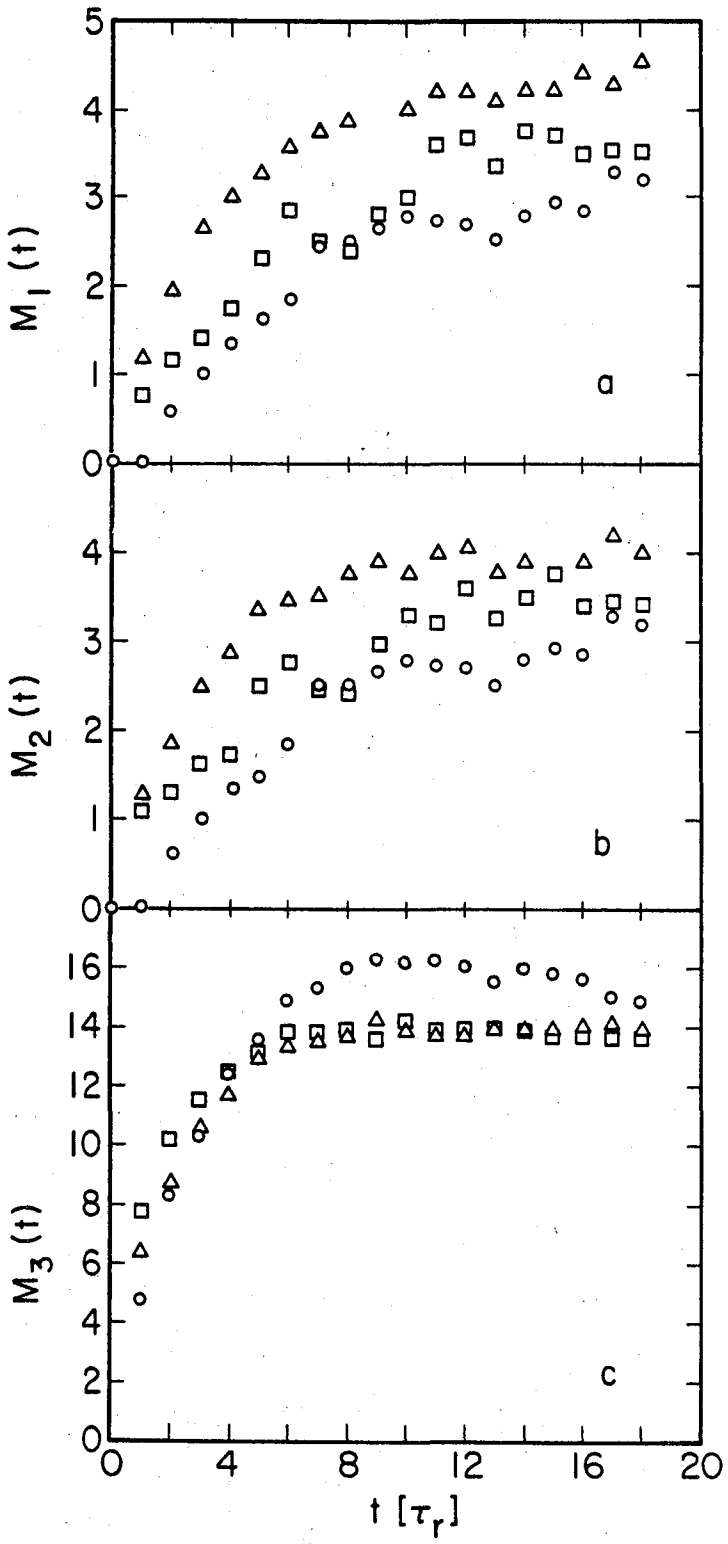

Fig. 6

XBL 805-9692

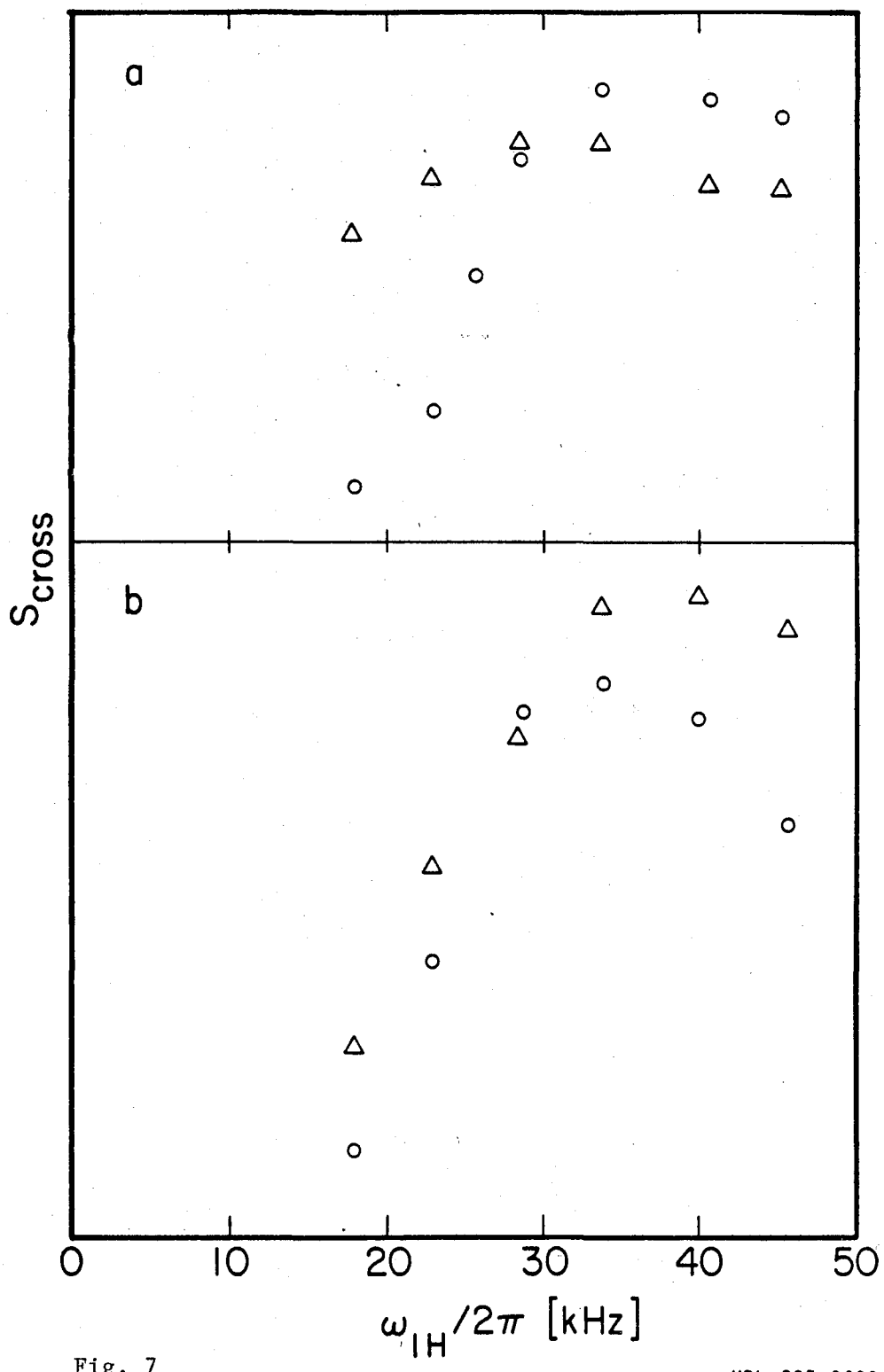

Fig. 7

XBL 805-9690

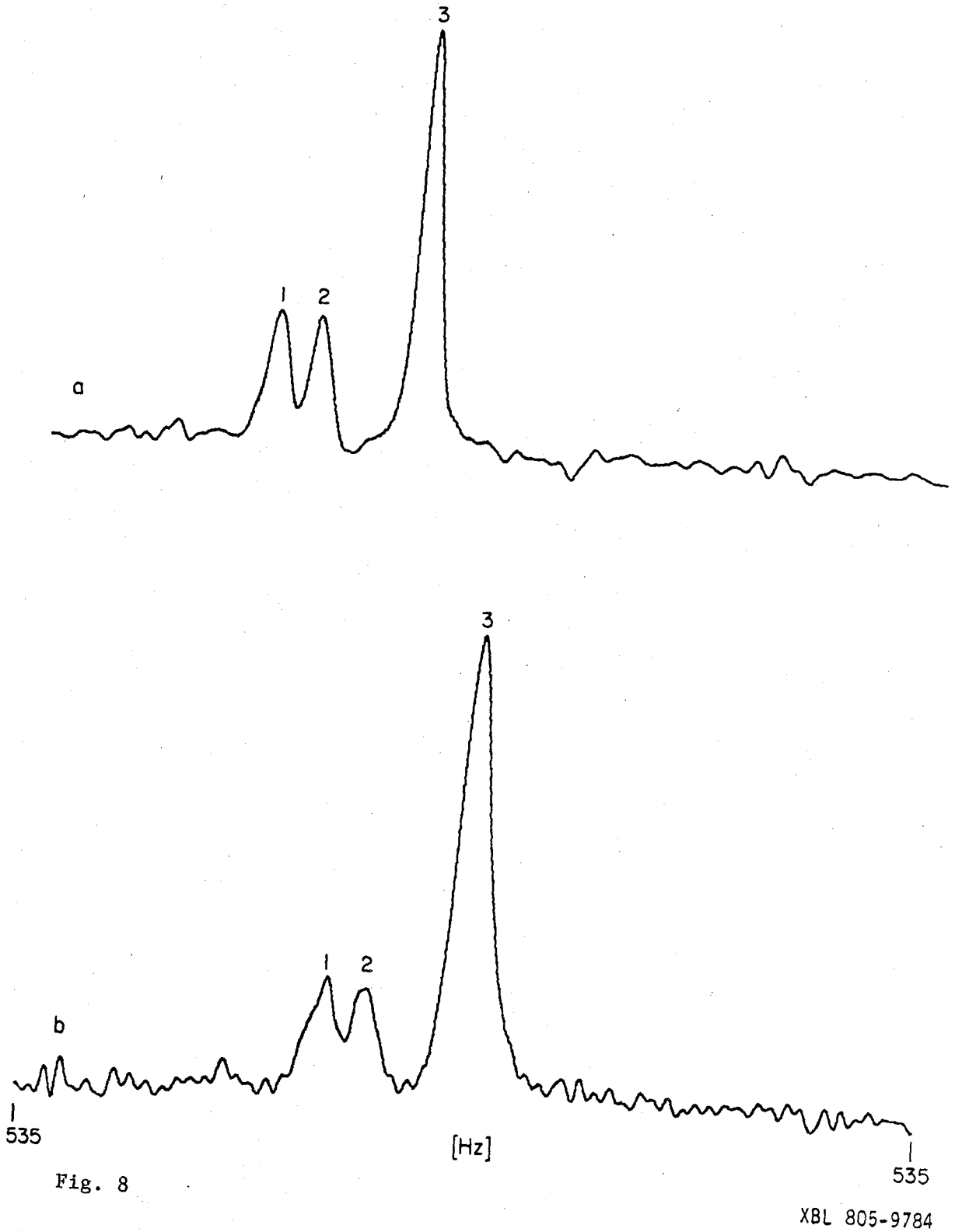

Fig. 8

XBL 805-9784